Cellular Signalling 59 (2019) 76–84

Contents lists available at ScienceDirect

Cellular Signalling

journal homepage: www.elsevier.com/locate/cellsig

The γ-secretase inhibitor GSI-I interacts synergistically with the proteasome inhibitor bortezomib to induce ALK+ anaplastic large cell lymphoma cell apoptosis

Qingxiu Dang[1], Lili Chen[1], Mengqi Xu[1], Xuefen You, Hong Zhou, Yaping Zhang*, Wenyu Shi*

Department of Hematology, Affiliated Hospital of Nantong University, Nantong 226001, Jiangsu, China

ARTICLE INFO

Keywords:
Anaplastic large cell lymphoma
γ-secretase inhibitor
Proteasome inhibitor
Synergistic effect
Apoptosis

ABSTRACT

Single agent treatment of the γ-secretase inhibitor (GSI-I) or proteasome inhibitor in anaplastic lymphoma kinase positive anaplastic large cell lymphoma (ALK+ ALCL) shows limited response and considerable toxicity. Here, we examined the effects of the combination of low dose GSI-I and the proteasome inhibitor bortezomib (BTZ) in ALK+ ALCL cells *in vivo* and *in vitro*. We found that ALK+ ALCL cells treated with the BTZ and GSI-I combination treatment showed elevated apoptosis, consistent with increased caspase activation, compared with BTZ or GSI-I alone. The combination treatment also inhibited AKT and extracellular signal-related kinase pathways, as well as stress-related cascades, including the c-jun N-terminal kinase and stress-activated kinases. Moreover, combined treatment in a murine xenograft model resulted in increased apoptosis in tumor tissues and reduced tumor growth. Our results reveal the synergistic anti-tumor effects of low dose inhibitors against γ-secretase and the proteasome and suggest the potential application of the tolerable BTZ/GSI-I combined agents in treating ALK + ALCL in future clinical treatment.

1. Introduction

Anaplastic large cell lymphoma (ALCL) is an aggressive subtype of non-Hodgkin's lymphoma (NHL) that is derived from CD4+ T cells [1]. Systemic ALCL is classified into two subtypes based on the presence or absence of chromosomal translocations of the anaplastic lymphoma kinase (ALK) gene at the 2p23 locus [2,3]. The t (2;5) (p23;q35) translocation in ALCL encodes for the nucleophosmin-ALK (NPM-ALK) fusion protein [4], which interacts with survival pathways to promote cell proliferation, anti-apoptosis and tumor formation [5,6]. Although many patients with ALCL can obtain complete remission with conventional chemotherapy, relapse still frequently occurs and these patients eventually show poor clinical outcome [7,8]. Recent studies on the pathogenesis of malignant T-cell tumors have identified several mechanisms, including abnormal regulation of cellular apoptosis and proliferation and the dysregulation of a variety of signaling pathways, including extracellular signal-regulating kinase 1/2 (ERK1/2) [9,10], nuclear factor (NF)-κB [11,12], AKT/mTOR [9,13], p38 mitogen-activated protein kinase (p38 MAPK) [14], and c-jun N-terminal kinase (JNK/c-Jun) [15]. The identification of new regimens for the treatment of ALK+ ALCL is critical to improve patient outcome, especially non-chemotherapeutic regimens that specifically target these pathways.

Studies have demonstrated that irregular activation of the Notch1 pathway is involved in driving tumorigenesis of various cancers. Notch1 signaling regulates cell proliferation and differentiation, and aberrant Notch1 signaling plays a critical role in cancer progression [16]. The γ-secretase is complex protease that contains several transmembrane domains, a catalytic subunit and accessory subunits [17]. Several studies showed that γ-secretase can activate Notch receptors, and thus the development of γ-secretase inhibitors (GSIs) has attracted increasing interest [18]. Indeed, some reports demonstrated that GSIs can prevent activation of the Notch1 signaling pathway [19]. GSIs have been used to block the progression of Alzheimer's disease [20], and Notch1 inhibition by GSIs can be effective in cancers such as hepatocellular carcinoma, gastric cancer, neuroblastoma and others [21]. Moreover, GSIs have shown efficacy against diffuse large B cell lymphoma and mantle cell lymphoma [22]. In NHL, including ALK+ ALCL, GSIs can inhibit proliferation *in vitro* and induce apoptosis, accompanied with downregulation of cyclin D1, Bcl-xL and XIAP [23]. However, GSIs can cause toxic side effects, including inflammation and gastrointestinal issues [24].

Inhibitors against the proteasome, a component of the ubiquitin-

* Corresponding authors.
E-mail addresses: zzyaping@163.com (Y. Zhang), shiwenyu@ntu.edu.cn (W. Shi).
[1] Co-first author: These authors contributed equally to this work.

https://doi.org/10.1016/j.cellsig.2019.03.013
Received 29 October 2018; Received in revised form 11 March 2019; Accepted 12 March 2019
Available online 14 March 2019
0898-6568/

proteasome pathway that degrades cellular proteins, provide a new strategy for targeting the 26S proteasome [25]. Proteasome inhibitors can exhibit potent anti-cancer effects against different tumor cells and were shown to induce apoptosis in pancreatic, renal, prostate and squamous cell carcinomas *in vivo* and *in vitro* [26]. Bortezomib (BTZ) is a proteasome inhibitor that can regulate canonical as well as non-canonical NF-κB signaling [27]. Another anti-tumor mechanism of BTZ may be associated with the upregulation of NOXA [28]. In addition to BTZ regulation of NF-κB and NOXA, BTZ has a variety of targets in malignant cells, such as caspase-8 and caspase-9 [29]. cFLIP can block the activation of caspase-8 to inhibit apoptosis [30]. However, BTZ is associated with various systemic toxicities in patients, including vomiting, nausea, diarrhea and constipation, as well as peripheral neuropathy and other effects [31].

Previous studies have shown that a combination of proteasome inhibitor and histone deacetylase exhibits synergistic effects against malignant tumors, including multiple myeloma, chronic lymphocytic leukemia and mantle cell lymphoma [32–34]. Other studies showed anti-cancer effects with the combination of GSIs with other agents [35]. Several reports have shown a synergetic anti-cancer effect from BTZ in combination with other chemotherapeutic agents, suggesting a promising role for BTZ in combined therapy regimens [36]. However, no studies have examined the potential therapeutic effects of the combination of BTZ and GSIs in ALK+ ALCL. Because of the limitations using γ-secretase or proteasome inhibitors as single agents in treating ALK+ ALCL, we hypothesized that combining both inhibitors may be a superior and safer strategy to treat ALK+ ALCL than each agent alone. In this study, we examined the effects of the combination of BTZ with GSI-I in ALK+ ALCL *in vivo* and *in vitro* and explored the therapeutic mechanism.

2. Materials and methods

2.1. Cell lines and reagents

This study included four ALK+ ALCL cell lines: Karpas 299, SR-786, DEL and SU-DHL-1 (DSMZ, Braunschweig, Germany). Cells were maintained in RPMI-1640 medium (Gibco, USA), supplemented with 20% heat-inactivated fetal bovine serum (FBS, Sigma Aldrich, St. Louis, MO, USA) and maintained at 37 °C with 5% CO_2. GSI-I was purchased from Sigma (USA) and the proteasome inhibitor BTZ was obtained from Selleckchem (Houston, TX, USA).

2.2. BTZ and GSI-I treatments

We examined the effects of the combination of low dose, inhibiting the cellular proliferation of 20–30%, GSI-I and BTZ based on our isobologram studies to ensure drug availability and fewer side effects in ALK+ ALCL cells *in vivo* and *in vitro*. Karpas 299, SR-786, DEL and SU-DHL-1 cells were treated with GSI-I at 2.0 μmoL, 1.5 μmoL, 2.5 μmoL, 2.0 μmoL with or without BTZ 5.0 nmoL.

2.3. Cell viability assay

Cell viability was analyzed using the MTS Kit (G3580; Promega, USA) according to the manufacturer's protocol. Four treatment groups were established for each cell line: control group, GSI-I group, BTZ group and GSI-I + BTZ group. Cells were seeded into 96-well plates at a concentration of 1×10^6 cells/well and incubated in the presence of GSI-I 2.0 μmoL, 1.5 μmoL, 2.5 μmoL, 2.0 μmoL and/or with BTZ 5.0 nmoL at 37 °C for 48 h. The MTS reagent was added and cells were incubated at 37 °C for 4 h, followed by detection of the absorbance value (OD) at 490 nm using a microplate reader to evaluate the cell growth inhibition rate.

2.4. Isobolographic analysis

Based on concentration-response curves obtained from the *in vitro* treatments of cell lines, three isoeffect curves were generated using isobolograms to determine the effects (synergistic *vs.* additive *vs.* antagonistic) of the combination of BTZ and GSI-I. Concentration-dependent effects were calculated by MS-Excel (Microsoft; Redmond, WA, USA) for one drug while keeping constant concentrations for the other.

2.5. Cell proliferation assay

Cell proliferation was measured by using the BrdU cell proliferation kit (X1327K1, Exalpha Biologicals, Shirley, MD, USA) according to the manufacturer's protocol. After treatment with GSI-I and/or BTZ for 24 h and 48 h, cells were plated at a concentration of 2×10^6 cells/mL in 96-well plates. Twenty microliters of BrdU (diluted 1:500) was added and cells were incubated overnight. The Fixing Solution was then added and plates were washed. Anti-BrdU monoclonal antibody was added (100 μL/well), followed by peroxidase goat anti-mouse Ig-G conjugate (diluted 1:2000; 100 μL/well). The plates were washed, and TMB substrate (100 μL/well) was added. Stop solution (50 μL) was added and plates were read in an ELISA plate reader (450/595 nm).

2.6. Apoptosis assay

Apoptosis was examined using a flow cytometry kit (556547, BD Biosciences, CA, USA) after treatment for 24 h, according to the manufacturer's instructions. Cells were dual-stained with Annexin V and PI and then examined by flow cytometry (BD FACSCalibur system). Percentages of apoptotic cells were quantified using FlowJo software (BD Biosciences).

2.7. Anchorage-independent colony formation assay

Cells were plated in a methylcellulose-based medium (Methocult H4230, Stemcell Technologies) and mixed with RPMI-1640 medium at a ratio of 1:4 (v/v) after treatment for 24 h and 48 h. Cells were then harvested and mixed with methylcellulose in a 1:20 (v/v) ratio in 15 mL conical tubes. The contents were poured into 12-well plates, and plates were incubated at 37 °C in a 5% CO_2 incubator for 7 days. Colonies were visualized using the FluorChem 8800 imaging system (Alpha Innotech, San Leandro, CA, USA).

2.8. Antibodies

The following antibodies were used in this study: cleaved PARP (5625S), cleaved caspase-3(9661S), p-AKT(Ser473, 4051), PARP (9542P), cleaved Notch1(NICD, 4147S), Notch1(3608S), p-ERK (4370S), mTOR(7C10), p-mTOR(sRE2448), JNK(56G8), p-JNK(81E11), c-Jun(60A8), p-c-Jun(Ser73), caspase-8(1C12), cleaved caspase-8(18C8) and β-actin(8H10D10) (from Cell Signaling Technology, USA); Bcl-2 (sc-7382), ERK (sc-94), and caspase-3 (sc-7272) (from Santa Cruz Biotechnology, TX, USA); Bcl-xL(18-0217) (Zymed Laboratories, CA, USA); and cFLIP(ab8421) (Abcam, UK).

2.9. Western blotting

Protein samples (50 μg/well) from total cell lysates were electrophoresed on 10% SDS/PAGE and transferred to membranes. Membranes were blocked with 5% non-fat milk (100 mL 0.1% Tween 20/PBS with 5 g nonfat milk). Membranes were then incubated with specific primary antibodies at 4 °C overnight, followed by incubation with secondary antibodies. β-actin antibody served as the loading control. The immunocomplexes were visualized using an enhanced chemiluminescence detection system. Band density was quantified by the ImageJ analysis system (Wayne Rasband; National Institutes of

Health, USA). All of the primary antibodies were used at dilution 1:1000; the secondary antibodies were used at 1:5000 dilution.

2.10. Animal model

The experimental protocols were approved by the Animal Ethical Committee at Nantong University. SCID/beige mice (5- to 6-week-old females; Shanghai Laboratory Animal Center, Shanghai, China) were injected subcutaneously with 5×10^6 SR-786 cells in the right shoulder. When the tumors reached 50 mm^3, the mice were randomly divided into four groups ($n = 5$ per group): the control group (intraperitoneal, i.p., injection of PBS), GSI-I group (i.p.: 5 mg/kg/d over 14 days; two cycles, 5 days on and 2 days off), BTZ group (i.p.: 60 μg/kg once per day for 14 days) and GSI-I + BTZ combination group. We monitored tumor growth and measured the tumor volumes every 2 days using the formula $a^2 \times b \times 0.5$, in which a: width and b: length. Animals were sacrificed by cervical dislocation; we performed body necropsy and fixed the tumors in 10% buffered formalin or snap-froze tumors in liquid nitrogen. The weight of the experimental mice was about 20 g. During the experiment, the mice showed no significant change in body weight, indicating that they could tolerate the treatments.

2.11. Terminal deoxynucleotidyl transferase dUTP nick-end labeling (TUNEL) assay

Apoptosis in the tumor tissues from mice xenografts was evaluated using the TUNEL assay. *In situ* cellular apoptosis was determined by detecting DNA fragments in formalin-fixed sections (5.0 μm) from mice lymphoma xenografts.

2.12. Statistical analysis

We conducted statistical analyses by one-way ANOVA, and multiple comparison between the groups was performed using Bonferroni by SPSS 21.0. Two-way ANOVA with post-hoc analysis by Sidak's multiple comparisons test was applied to mouse tumor growth. Data are expressed as means ± SE using GraphPad Prism software 8.0.1 (CA, USA). $P < .05$ was considered statistically significant.

3. Results

3.1. Combination of BTZ and GSI-I induces synergistic inhibitory effects in ALK+ ALCL cells

To investigate the effects of combined treatment of BTZ and GSI-I, we first treated four ALK+ ALCL cell lines, Karpas 299, SR-786, DEL and SU-DHL-1, with different concentrations of BTZ and/or GSI-I for 48 h. Treatment with only BTZ or GSI-I resulted in a concentration-dependent decrease in cell viability of all four ALK+ ALCL cell lines (Fig. 1A, B). Notably, the combination therapy was more potent in inhibiting ALK+ ALCL cell viability compared with the single agent treatment. Single treatment of either 10.0 nM BTZ or 3.5 μM GSI-I induced an approximately 60% reduction in DEL cell viability, while the combination treatment resulted in a 90% decrease in DEL cell viability (Fig. 1C).

We next performed isobologram analysis to evaluate whether the combination treatment of BTZ and GSI-I showed synergistic or additive effects. Plotting isoeffect curves for the drugs produces an overlapping area defined as the additive envelope (Fig. 1D). When the data points of the drug combination fall within the envelope, the effect of the combination drug treatment is regarded as additive; when the data points fall to the left of the envelope, the effect of the combination drug treatment is considered synergistic. Isobologram analysis revealed that most of the data points were located to the left of the envelope, indicating a synergistic effect of BTZ and GSI-I.

3.2. Combination of BTZ and GSI-I decreases proliferation and induces apoptosis of ALK+ ALCL cell lines

We next examined the biological effects of γ-secretase or proteasome inhibitors, alone and together, by treating the ALK+ ALCL cell lines with different concentrations of BTZ and/or GSI-I for 24 h or 48 h. We first evaluated cell proliferation using BrdU assay (Fig. 2A). Proliferation was inhibited after 24 h of co-exposure, which was enhanced with the increasing co-exposure time. For example, GSI-I alone induced a 5–10% and 10–20% reduction in cell proliferation while BTZ induced a 10–40% and 30–60% reduction in cell proliferation at 24 h and 48 h, respectively. However, the combination treatment achieved a 40–70% and 60–90% inhibition of proliferation at 24 h and 48 h of treatment.

We also examined the influence of BTZ and/or GSI-I on apoptosis using Annexin V-FITC/PI dual staining and flow cytometric analysis. We detected significantly increased apoptosis in response to the combined treatment compared with individual treatments. After 24 h, the percentage of apoptotic cells (both early and late apoptosis) in response to the combination treatment was 20.88% in Karpas 299 cells, 22.05% in SR-786 cells, 25.57% in DEL cells and 31.65% in SU-DHL-1 cells, which were significantly higher apoptotic rates than in cells treated with BTZ alone (11.10%, 11.07%, 8.81% and 15.72%, respectively) or GSI-I alone (11.94%, 9.76%, 9.87% and 13.22%, respectively) (Fig. 2B, C).

We also performed clonogenic assays to analyze effects of BTZ and/or GSI-I on ALK+ ALCL cell colony formation (Fig. 2D, E). While BTZ or GSI-I alone resulted in decreased colony numbers, the combined treatment caused a more dramatic reduction in the number of Karpas 299 and DEL cell colonies. Furthermore, after 24 h of the combined treatment of BTZ and GSI-I, the number of colonies was about 40–50, while only 15–20 colonies were observed after 48 h of treatment.

3.3. Combination of BTZ and GSI-I regulates signaling pathways in ALK+ ALCL cell lines

We next investigated the effect of BTZ and/or GSI-I on molecular pathways associated with apoptosis in Karpas 299 and DEL cells (Fig. 3A). Treatment with BTZ or GSI-I slightly increased cleaved caspase-3, cleaved caspase-8 and cleaved PARP levels, as well as decreased Bcl-2 and Bcl-xL which is consistent with the induction of apoptosis, with no significant influence on the total protein levels. However, the combination of BTZ and GSI-I led to a slight reduction in total caspase-3 and PARP. In Karpas 299 cells, BTZ and/or GSI-I decreased cFLIP expression, while BTZ had no significant effects on the expression of cFLIP in DEL cells. These molecular changes are consistent with the flow cytometry results showing increased apoptosis in response to the combination treatment.

We also examined the effect of BTZ and/or GSI-I on the AKT/mTOR and ERK pathways (Fig. 3B). Single treatment with BTZ or GSI-I caused a slight decrease in p-ERK levels, as well as a notable reduction in p-AKT and p-mTOR levels. However, the combined treatment significantly decreased the levels of p-ERK, p-AKT and p-mTOR in both cell lines compared with the single treatments. No changes were detected in total ERK, AKT and mTOR protein levels.

To analyze the impact of BTZ and/or GSI-I on Notch1 signaling, we examined the expressions of cleaved Notch1, Notch1 and the Notch1 targets Hes-1 and c-Myc (Fig. 3C). BTZ or GSI-I alone reduced cleaved Notch1 and Notch1 expression. Moreover, the expressions of c-Myc and Hes-1 were slightly decreased after treatment with GSI-I or BTZ. However, we observed stronger downregulation of cleaved Notch1, Notch1 and the Notch1 targets in response to the combined treatment with BTZ and GSI-I compared with either single treatment alone.

Finally, we evaluated the influence of BTZ and/or GSI-I on JNK/c-Jun pathway proteins (Fig. 3D). Either BTZ or GSI-I increased p-JNK, p-c-Jun and p-p38 levels. However, the combination treatment strongly increased p-JNK, p-c-Jun and p-p38 expression compared with either

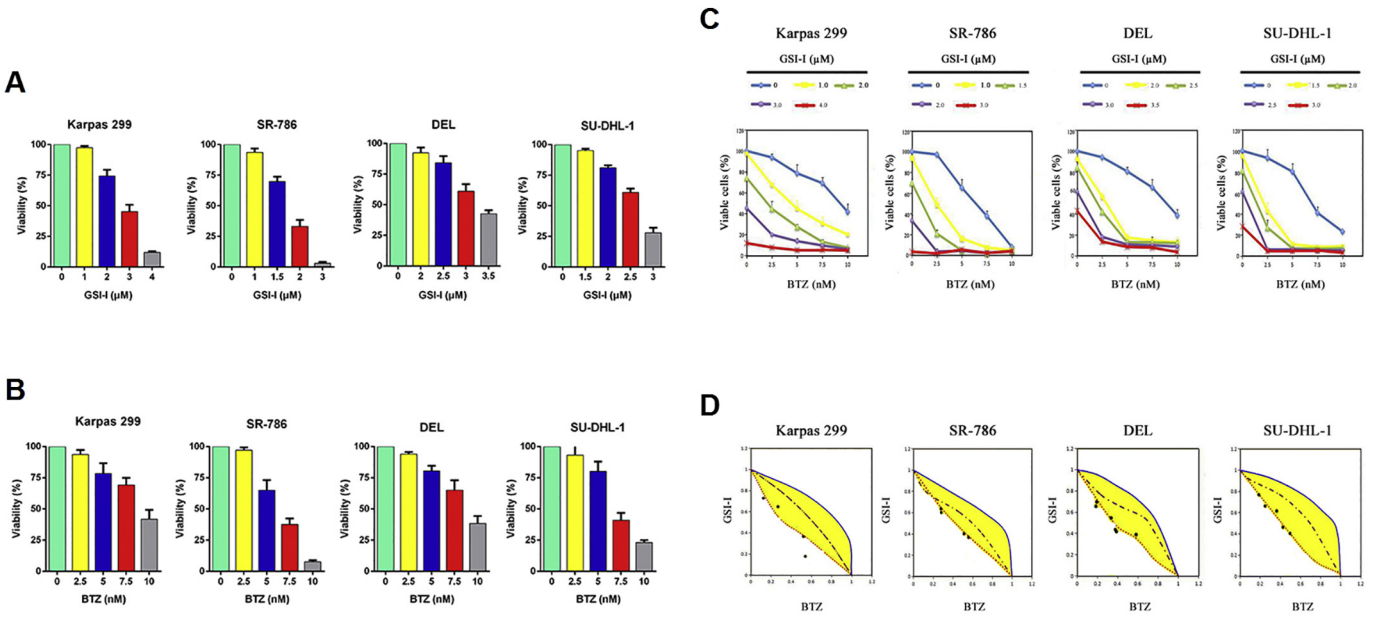

Fig. 1. Combination of BTZ + GSI-I *vs.* BTZ and GSI-I induces synergistic inhibitory effects in ALK+ ALCL cells. (A, B). Karpas 299, SR-786, DEL and SU-DHL-1 cells were treated with the indicated concentrations of GSI-I and BTZ for 48 h. Data represent means ± SE of three independent experiments. (C). Compared with a single agent, combined treatment with BTZ + GSI-I *vs.* BTZ and GSI-I led to significant reduction in viability of Karpas 299, SR-786, DEL, and SU-DHL-1. (D). Isobolographic curves demonstrate that most of the data points are lying to the left of the envelope of additivity (yellow area), illustrating that combining BTZ + GSI-I *vs.* BTZ and GSI-I induces synergistic effects in ALK+ ALCL cells. (For interpretation of the references to colour in this figure legend, the reader is referred to the web version of this article.)

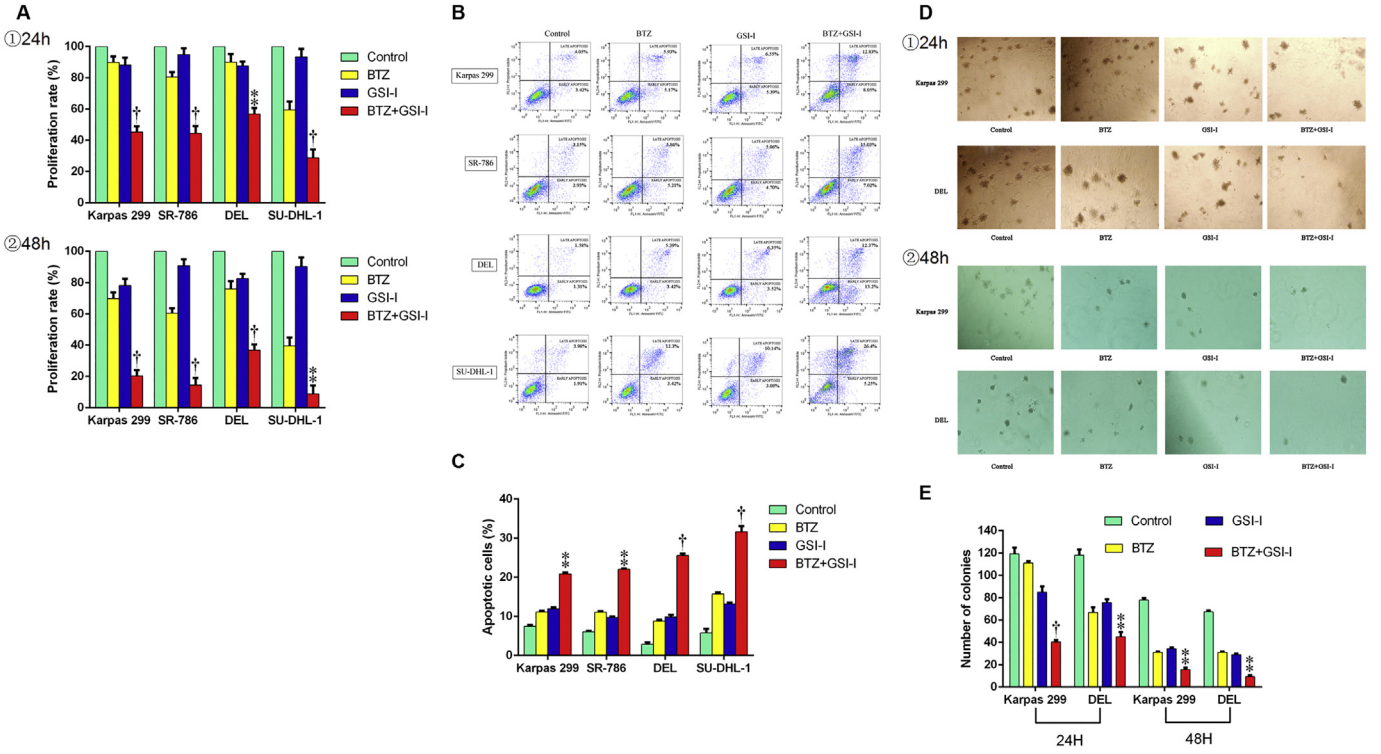

Fig. 2. Combination of BTZ and GSI-I decreases proliferation and induces apoptosis of ALK+ ALCL cells lines. Karpas 299, SR-786, DEL and SU-DHL-1 were treated with GSI-I 2.0 μmoL, 1.5 μmoL, 2.5 μmoL, 2.0 μmoL and/or with BTZ 5.0 nmoL. (A). Proliferation rate of cells is shown by BrdU after 24 and 48 h. (B). Apoptotic rate is studied using Annexin V-FITC/PI dual staining and flow cytometric analysis after 24 h. Representative flow cytometry data are shown. Accordingly, the percentages of late apoptotic cells (right upper panel) and earlier apoptotic cells (right lower panel), are significantly increase in combined treatment. (C). Quantification of the results from B (right upper and lower quadrants). (D). Representative examples of colonies from the Karpas 299 and DEL cell lines with and without treatment with BTZ and/or GSI-I for 24 or 48 h. (E). Whereas BTZ or GSI-I decreased the colony formation of Karpas 299 and DEL cells in methylcellulose, their combined effects were much more dramatic. Representative examples of the colonies after treatment with different regimens. (Data represent means ± SE of three independent experiments. ‡:$P < .01$, †:$P < .001$, BTZ + GSI-I *vs.* BTZ and GSI-I).

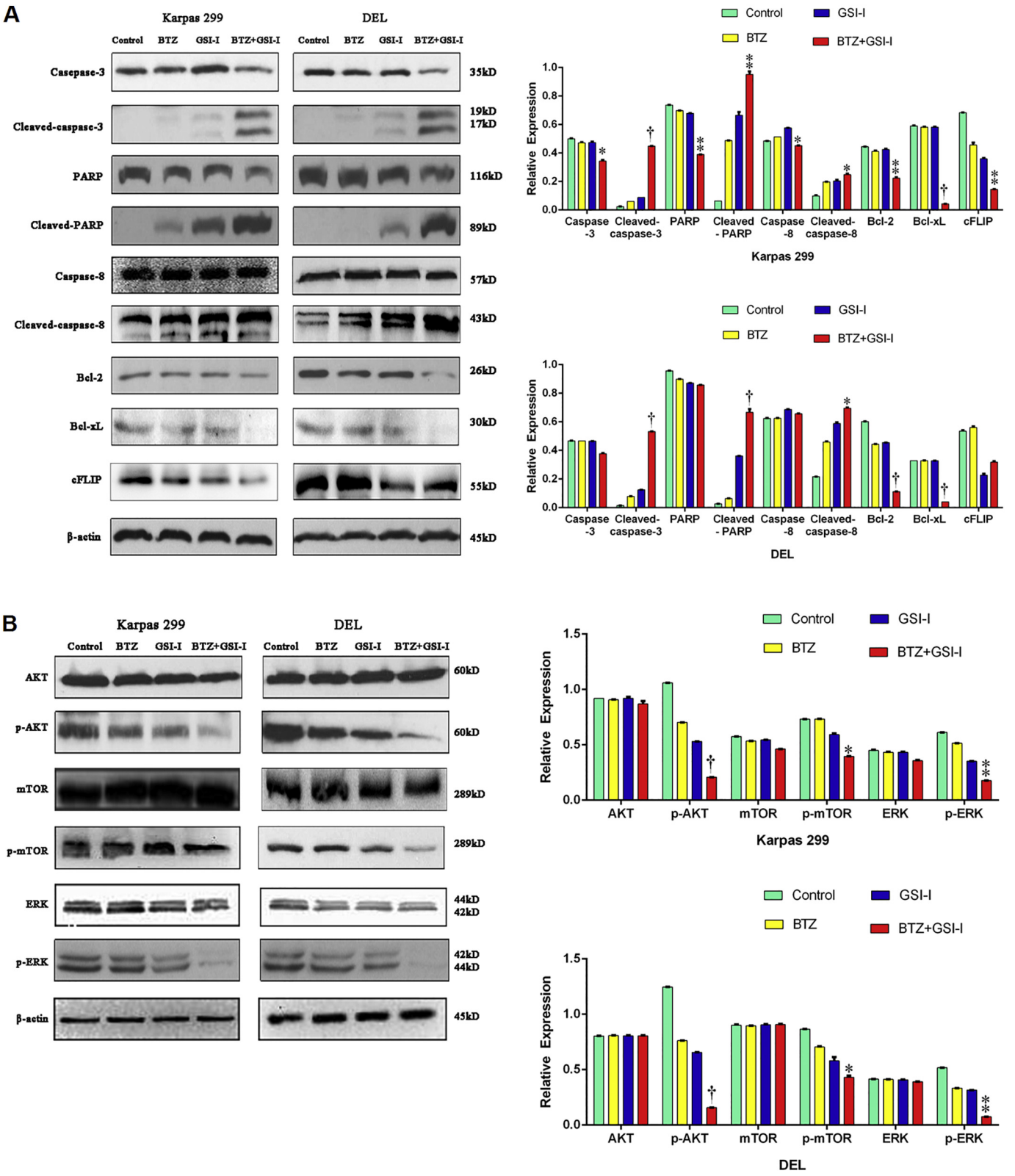

Fig. 3. Combination of BTZ and GSI-I regulates signaling pathways in ALK + ALCL cell lines. Karpas 299 and DEL were treated with GSI-I 2.0 μmoL, 2.5 μmoL and/or with BTZ 5.0 nmoL for 48 h. The interference efficiencies of BTZ and/or GSI-I were measured by western blot analysis. β-actin was used as a control for protein loading and integrity. (A). Treatment of Karpas 299 and DEL cells with BTZ + GSI-I *vs.* BTZ and GSI-I activates the cleavage of caspase-3, caspase-8 and PARP, as well as decreases Bcl-2 and Bcl-xL, which is consistent with the occurrence of apoptosis. The effects of the combined treatment were more pronounced than the effects of a single agent. (B). p-AKT, p-mTOR and p-ERK were markedly decreased after the combination treatment compared with the single agent. (C). Treatment with BTZ + GSI-I *vs.* BTZ and GSI-I decreased cleaved-Notch1, c-Myc and Hes-1 immensely. (D). The levels of p-JNK, p-c-Jun and p-p38 was upregulated after treated with BTZ and/or GSI-I. (Data represent means ± SE of three independent experiments. *:$P < .05$, ‡:$P < .01$, †:$P < .001$, BTZ + GSI-I *vs.* BTZ and GSI-I).

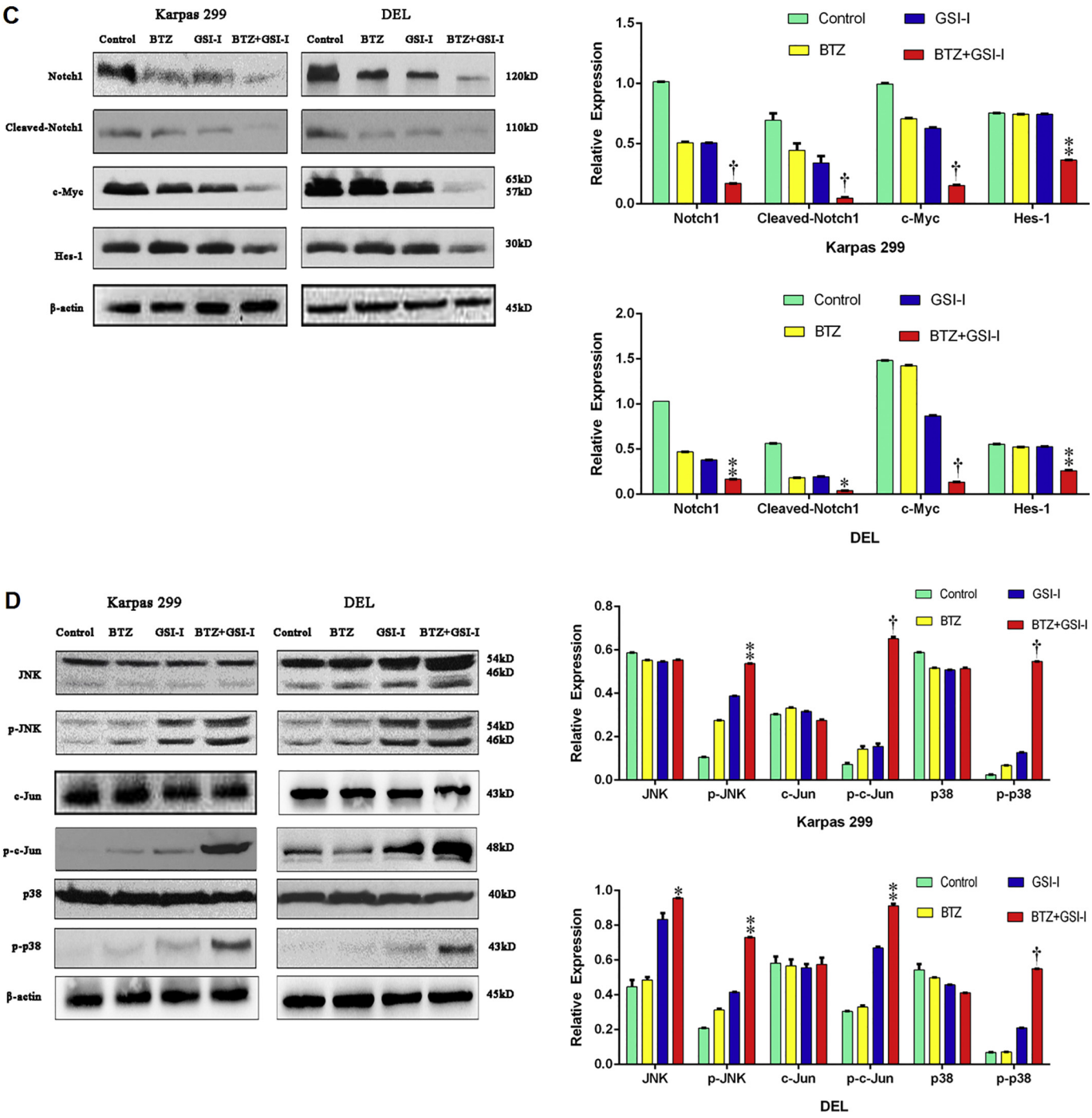

Fig. 3. (*continued*)

single treatment alone. No changes in JNK, c-Jun and p38 levels were observed in Karpas 299 cells in response to any treatment and no changes in c-Jun and p38 were observed in DEL cells. We did observe increased JNK in DEL cells with BTZ and/or GSI-I, which was consistent with the results of Zhang et al. [37].

3.4. Combination of BTZ and GSI-I suppresses ALK+ ALCL xenograft tumor growth in mice

We next evaluated the potential therapeutic effect of the BTZ and GSI-I combination treatment on ALK+ ALCL cells in a mouse model *in vivo*. SR-786 cells were subcutaneously injected in the right shoulder of SCID/beige mice, resulting in the formation of tumors. Mice were treated with either single agent alone or the combination treatment. The BTZ and GSI-I combination inhibited tumor growth more notably than the individual agents (Fig. 4A). While the single BTZ or GSI-I treatment significantly inhibited growth by day 11 compared with controls, the combined treatment group showed significant inhibition of tumor growth on day 9 (Fig. 4B). By day 15, we observed smaller tumor sizes in the mice treated with the BTZ and GSI-I combination than those treated with BTZ or GSI-I alone. Kaplan-Meier survival curves indicated that mice treated with combined treatments had superior overall survival compared with mice treated with BTZ or GSI-I (Fig. 4C). TUNEL staining in tumor tissues revealed a larger number of apoptotic cells in the tumors treated with the combination therapy compared with tumors from the control and individual treatment

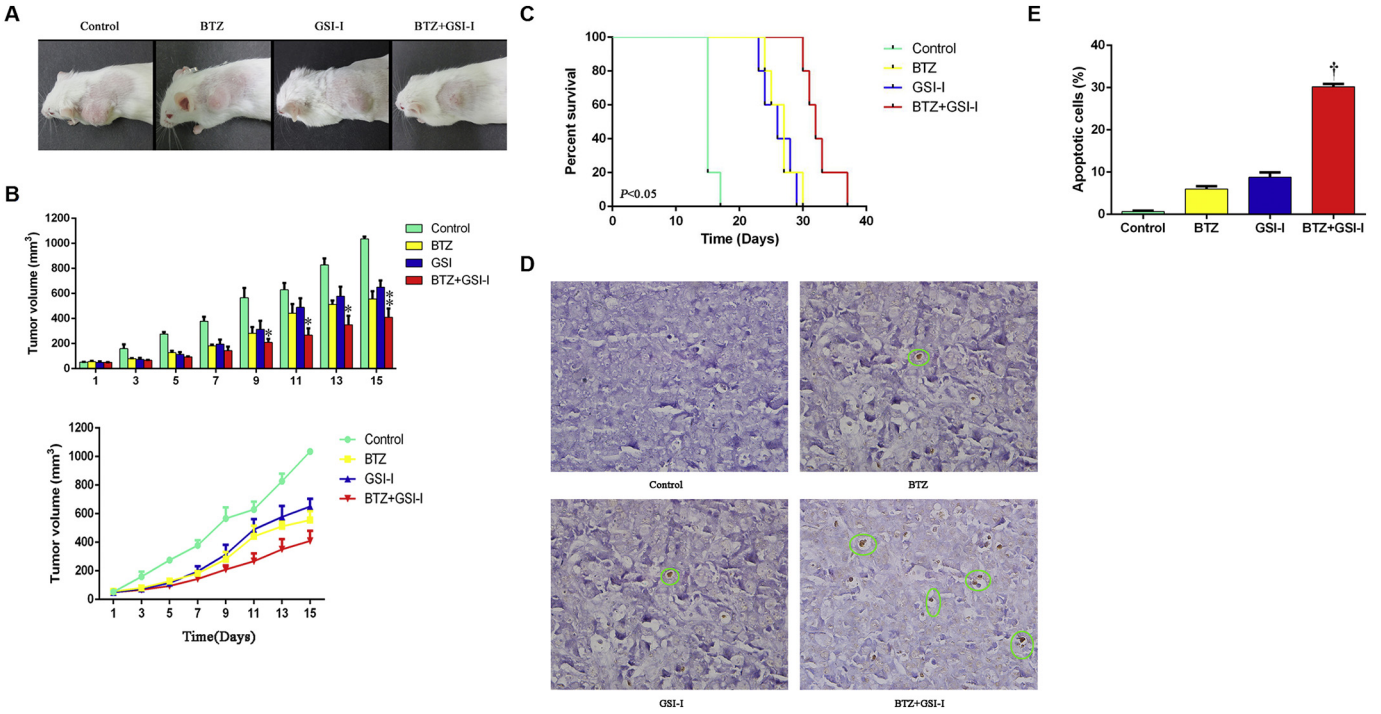

Fig. 4. Combination of BTZ and GSI-I suppresses ALK+ ALCL xenograft tumor growth in mice. (A). Mice were subcutaneously injected with SR-786 cells and then treated with BTZ, GSI-I or the combination treatment as described in Methods. Representative images of mice and tumors on day 14 are shown. (B). Quantitative analysis of tumor volume indicates that the combination treatment was superior to treatment with a single drug in suppressing tumor growth. For example, combined treatment with GSI-I and BTZ significantly inhibited tumor growth starting from day 9 after treatment compared with controls. Single GSI-I or BTZ treatment showed significant inhibitory effects compared with controls at day 11 ($P < .05$). Compared with the single treatment, the combination of GSI-I and BTZ inhibited tumor growth. (C). Kaplan–Meier analysis demonstrated that mice with the combined treatment had a significantly better prognosis than those with single treatment or the control. ($P < .05$, log-rank test). (D, E). Representative images of TUNEL staining in tumor tissues from the different treatment groups. (Data represent means ± SE of three independent experiments. *:$P < .05$, ‡:$P < .01$, †:$P < .001$, BTZ + GSI-I *vs.* BTZ and GSI-I).

groups (Fig. 4D). During the experiment, the mice in all groups showed no significant change in body weight, indicating that they could tolerate the experimental treatment.

4. Discussion

Our study reveals the effect of the combination treatment of GSI-I with BTZ on ALK+ ALCL both *in vivo* and *in vitro*. We examined the effects of the combination of low dose BTZ and GSI-I based on isobologram studies ensuring drug availability and fewer side effects in ALK+ ALCL cells *in vivo* and *in vitro*. Our results indicated that the combination treatment of BTZ and GSI-I inhibited cell proliferation and promoted apoptosis in ALK+ ALCL cell lines more potently than the single treatments alone.

Our understanding of the biological function of apoptosis has evolved from its role as mechanism for “programmed cell death” to acting as a barrier against malignancy [38]. Studies have demonstrated that the apoptosis programmed cell death pathway serves as mechanism to block cancer development [39], and the mechanisms of apoptosis and the strategies used by cancer cells to evade apoptosis have been intensively explored over the last decade. Apoptosis is induced through the activation of a cascade of normal latent proteases, including effector caspases (caspase-8 and caspase-9). Currently, the intrinsic apoptotic process is considered to be the main defense for the pathogenesis of cancer [38]. Consistent with the induction of apoptosis by the combination treatment, we observed increased production of cleaved PARP, cleaved caspase-3, and cleaved caspase-8 production, which is consistent with the results of Chen et al. [40]. We also observed that BTZ and GSI-I reduced levels of Bcl-2, Bcl-xL and cFLIP. The anti-cancer activities of BTZ and GSI-I were further confirmed in the mouse model. Mice treated with the combination of BTZ and GSI-I demonstrated significant tumor regression compared with monotherapy or untreated controls.

Our findings indicated that multiple molecular mechanisms may be contributing to the synergistic effect between BTZ and GSI-I in ALK+ ALCL cells. Cytoprotective pathways, including ERK, Notch and AKT/mTOR, confer a survival advantage on ALK+ ALCL, not only rendering these tumors resistant to conventional cytotoxic drugs, but also protecting cells from apoptosis [5]. The Notch signaling pathway is a key pathway that regulates cell differentiation, proliferation and survival and plays a critical role in several developmental processes, such as neurogenesis, angiogenesis and hematopoiesis [41]. The multiple abilities of the Notch signaling pathway to inhibit or induce differentiation, to drive or arrest proliferation and to promote survival or induce apoptosis in a cell-specific way enables the Notch signaling pathway to promote or prevent tumor formation in a variety of cells [42]. Notch receptors are divided into four types, and abnormal Notch1 activation is associated with ALCL [43]. Moreover, the Notch1 pathway interacts with a number of oncogenic signaling pathways. Notch1 activates the PI3K/AKT signaling pathway [44,45], while AKT upregulates Notch1 *via* vascular endothelial growth factor [46]. The AKT signaling pathway and its interaction with Notch1 interaction maintain the survival of T lymphoproliferative tumors [47]. Notch1 also phosphorylates ERK1/2 and promotes tumor cell proliferation, and the ERK signaling pathway also promotes the Notch1 signaling pathway [48,49]. GSI-I modulates Notch1-mediated induction of target genes through blocking proteolytic activation of Notch1 [50].

In addition to inactivation of Notch, we found that the combination of BTZ and GSI-I downregulated ERK phosphorylation in ALK+ ALCL cells, and we speculate this may occur through the inhibition of upstream regulators of the ERK pathway. These findings emphasize the functional complementation of the two drugs in the inhibition of ERK

signaling. Recent studies have revealed the intersection between regulatory circuits that control apoptosis, autophagy and cell homeostasis. For example, signaling pathways involving PI3-kinase, mTOR kinases and AKT are stimulated by survival signals to hinder apoptosis; PI3K signaling is downregulated in the absence of survival signals, leading to apoptosis [51–53]. Notably, a cross-talk between the ERK and AKT cascades has also been recently described [54]. We found that the combination of BTZ and GSI-I could reduce AKT signaling; the level of phosphorylated AKT was reduced by the BTZ and GSI-I combination, suggesting a role in AKT signaling to downregulate the threshold of apoptosis. Recently, the relationship between ERK and AKT cascades was reported [55]. Therefore, downregulation of both the AKT/mTOR and ERK signaling pathways may be more fatal than interruption of either pathway alone in ALK + ALCL.

The c-Jun transcription factor plays an important role in the progression of many hematological diseases [56,57]. A previous study showed that BTZ upregulated the expression of p-JNK, a critical upstream messenger of c-Jun [58]. BTZ-mediated induction of apoptosis in leukemia cells has also been linked to JNK and p38 MAPK activation [59]. Our results showed that the combination of BTZ with GSI-I led to a significant increase in p-JNK and p-c-Jun, consistent with their activity as inhibitors of cell apoptosis, and these increases were marked compared with single treatments alone. Together these results indicate the synergic effect of the combination treatment on stress-related ALK + ALCL apoptosis cascades.

In conclusion, our study provides novel evidence that GSI-I in combination with BTZ synergistically inhibited ALK + ALCL cells *in vitro* and ALK + ALCL tumor growth *in vivo*. These findings may provide a new strategy for the clinical treatment of ALK + ALCL.

Acknowledgements

We thank Edanz Group (www.edanzediting.com/ac) for editing a draft of this manuscript.

Authors' contributions

WYS and YPZ conceived and designed the study. QXD, LLC, MQX, XFY and HZ performed the experiments and analyzed the data. WYS and QXD wrote and revised the manuscript. All authors read and approved the final manuscript.

Funding

The study was funded by the National Youth Science Foundation Project (NO. 81101786), the “Top Six Talents in Jiangsu Province” (NO. 2011-ws-062), the National Natural Science Foundation of China (NO. 81570184) and the Science and Technology Project of Nantong City (NO. MS12017003-2).

Conflict of interest

The authors declare that they have no conflict of interest.

Acknowledgements

The study was funded by the National Youth Science Foundation Project (NO. 81101786), the “Top Six Talents in Jiangsu Province” (NO. 2011-ws-062), the National Natural Science Foundation of China (NO. 81570184) and the Science and Technology Project of Nantong City (NO. MS12017003-2). We thank Edanz Group (www.edanzediting.com/ac) for editing a draft of this manuscript.

References

[1] C. Hoareau-Aveilla, T. Valentin, C. Daugrois, C. Quelen, G. Mitou, S. Quentin, J. Jia, S. Spicuglia, P. Ferrier, M. Ceccon, S. Giuriato, C. Gambacorti-Passerini, P. Brousset, L. Lamant, F.J.J.C.I. Meggetto, Reversal of microRNA-150 silencing disadvantages crizotinib-resistant NPM-ALK(+) cell growth, 125 (9) (2015) 3505–3518.
[2] A.J. Ferreri, S. Govi, S.A. Pileri, K.J. Savage, Anaplastic large cell lymphoma, ALK-negative, Crit. Rev. Oncol. Hematol. 85 (2) (2013) 206–215.
[3] M.T. Werner, Q. Zhang, M.A. Wasik, From pathology to precision medicine in anaplastic large cell lymphoma expressing anaplastic lymphoma kinase (ALK+ ALCL), Cancers 9 (10) (2017).
[4] M. Ceccon, M.E.B. Merlo, L. Mologni, T. Poggio, L.M. Varesio, M. Menotti, S. Bombelli, R. Rigolio, A.D. Manazza, F. Di Giacomo, C. Ambrogio, G. Giudici, C. Casati, C. Mastini, M. Compagno, S.D. Turner, C. Gambacorti-Passerini, R. Chiarle, C. Voena, Excess of NPM-ALK oncogenic signaling promotes cellular apoptosis and drug dependency, Oncogene 35 (29) (2016) 3854–3865.
[5] W. Shi, S.K. George, B. George, C.V. Curry, A. Murzabdillaeva, S. Alkan, H.M. Amin, TrkA is a binding partner of NPM-ALK that promotes the survival of ALK(+) T-cell lymphoma, Mol. Oncol. 11 (9) (2017) 1189–1207.
[6] M.T. Werner, C. Zhao, Q. Zhang, M.A. Wasik, Nucleophosmin-anaplastic lymphoma kinase: the ultimate oncogene and therapeutic target, Blood 129 (7) (2017) 823–831.
[7] A. Bazarbachi, D. Ghez, Y. Lepelletier, R. Nasr, H. de The, M.E. El-Sabban, O. Hermine, New therapeutic approaches for adult T-cell leukaemia, Lancet Oncol 5 (11) (2004) 664–672.
[8] M.C. Ferrufino-Schmidt, L.J. Medeiros, H. Liu, M.W. Clemens, K.K. Hunt, C. Laurent, J. Lofts, M.B. Amin, S. Ming Chai, A. Morine, A. Di Napoli, A. Dogan, V. Parkash, G. Bhagat, D. Tritz, A.E. Quesada, S. Pina-Oviedo, Q. Hu, F.J. Garcia-Gomez, J. Jose Borrero, P. Horna, B. Thakral, M. Narbaitz, R.C. Hughes 3rd, L.J. Yang, J.R. Fromm, D. Wu, D. Zhang, A.R. Sohani, J. Hunt, I.U. Vadlamani, E.A. Morgan, J.A. Ferry, R.C. Szigeti, T. J, R. Granados, S. Dertinger, F.A. Offner, A. Pircher, J. Hosry, K.H. Young, R.N. Miranda, Clinicopathologic features and prognostic impact of lymph node involvement in patients with breast implant-associated anaplastic large cell lymphoma, Am. J. Surg. Pathol. 42 (3) (2018) 293–305.
[9] M.R. Shurin, Y. Ma, A.A. Keskinov, R. Zhao, A. Lokshin, M. Agassandian, G.V. Shurin, BAFF and APRIL from activin A-treated dendritic cells upregulate the antitumor efficacy of dendritic cells in vivo, Cancer Res. 76 (17) (2016) 4959–4969.
[10] D. Naci, A. Fawzi, Alpha2beta1 integrin promotes T cell survival and migration through the concomitant activation of ERK/Mcl-1 and p38 MAPK pathways, Cell. Signal. 26 (9) (2014) 2008–2015.
[11] B. Martinez-Delgado, M. Cuadros, E. Honrado, A. Ruiz de la Parte, G. Roncador, J. Alves, J.M. Castrillo, C. Rivas, J. Benitez, Differential expression of NF-kappaB pathway genes among peripheral T-cell lymphomas, Leukemia 19 (12) (2005) 2254–2263.
[12] M.Q. Du, MALT lymphoma: a paradigm of NF-kappaB dysregulation, Semin. Cancer Biol. 39 (2016) 49–60.
[13] T. Wartewig, Z. Kurgyis, S. Keppler, K. Pechloff, E. Hameister, R. Ollinger, R. Maresch, T. Buch, K. Steiger, C. Winter, R. Rad, J. Ruland, PD-1 is a haploinsufficient suppressor of T cell lymphomagenesis, Nature 552 (7683) (2017) 121–125.
[14] J. Peng, J.Y. Tsang, D.H. Ho, R. Zhang, H. Xiao, D. Li, J. Zhu, F. Wang, Z. Bian, V.C. Lui, A. Xu, P.K. Tam, J.R. Lamb, H. Xia, Y. Chen, Modulatory effects of adiponectin on the polarization of tumor-associated macrophages, Int. J. Cancer 137 (4) (2015) 848–858.
[15] K.G. Guruharsha, M.W. Kankel, S. Artavanis-Tsakonas, The notch signalling system: recent insights into the complexity of a conserved pathway, Nat. Rev. Genet. 13 (9) (2012) 654–666.
[16] E.C. Hales, J.W. Taub, New insights into Notch1 regulation of the PI3K-AKT-mTOR1 signaling axis: targeted therapy of γ-secretase inhibitor resistant T-cell acute lymphoblastic leukemia, Cell. Signal. 26 (2014) 149–161.
[17] N. Oikawa, J. Walter, Presenilins and gamma-Secretase in membrane proteostasis, Cells 8 (3) (2019) pii: E209.
[18] A.D. Steg, M.R. Burke, H.M. Amm, A.A. Katre, Z.C. Dobbin, D.H. Jeong, C.N. Landen, Proteasome inhibition reverses hedgehog inhibitor and taxane resistance in ovarian cancer, Oncotarget 5 (16) (2014) 7065–7080.
[19] T. Na, J. Liu, K. Zhang, M. Ding, B.Z. Yuan, The notch signaling regulates CD105 expression, osteogenic differentiation and immunomodulation of human umbilical cord mesenchymal stem cells, PLoS One 10 (2) (2015) e0118168.
[20] S. Tagami, K. Yanagida, T.S. Kodama, M. Takami, N. Mizuta, H. Oyama, K. Nishitomi, Y.W. Chiu, T. Okamoto, T. Ikeuchi, G. Sakaguchi, T. Kudo, Y. Matsuura, A. Fukumori, M. Takeda, Y. Ihara, M. Okochi, Semagacestat is a pseudo-inhibitor of gamma-secretase, Cell Rep. 21 (1) (2017) 259–273.
[21] Y. Ran, F. Hossain, A. Pannuti, C.B. Lessard, G.Z. Ladd, J.I. Jung, L.M. Minter, B.A. Osborne, L. Miele, T.E. Golde, Gamma-secretase inhibitors in cancer clinical trials are pharmacologically and functionally distinct, EMBO Mol. Med 9 (7) (2017) 950–966.
[22] S. Tohda, T. Sato, H. Kogoshi, L. Fu, S. Sakano, N. Nara, Establishment of a novel B-cell lymphoma cell line with suppressed growth by gamma-secretase inhibitors, Leuk. Res. 30 (11) (2006) 1385–1390.
[23] T. Li, Y. Huang, S. Jin, L. Ye, N. Rong, X. Yang, Y. Ding, Z. Cheng, J. Zhang, Z. Wan, D.C. Harrison, I. Hussain, A. Hall, D.H. Lee, L.F. Lau, Y. Matsuoka, Gamma-secretase modulators do not induce Abeta-rebound and accumulation of beta-C-terminal fragment, J. Neurochem. 121 (2) (2012) 277–286.
[24] V. Ramakrishnan, S. Ansell, J. Haug, D. Grote, T. Kimlinger, M. Stenson, M. Timm, L. Wellik, T. Halling, S.V. Rajkumar, S. Kumar, MRK003, a gamma-secretase inhibitor exhibits promising in vitro pre-clinical activity in multiple myeloma and non-Hodgkin's lymphoma, Leukemia 26 (2) (2012) 340–348.
[25] R. Oerlemans, C.R. Berkers, Y.G. Assaraf, G.L. Scheffer, G.J. Peters, S.E. Verbrugge,

J. Cloos, J. Slootstra, R.H. Meloen, R.H. Shoemaker, B.A.C. Dijkmans, R.J. Scheper, H. Ovaa, G. Jansen, Proteasome inhibition and mechanism of resistance to a synthetic, library-based hexapeptide, Invest. New Drugs. 36 (5) (2018) 797–809.
[26] K. Tsumagari, Z.Y. Abd Elmageed, A.B. Sholl, E.A. Green, S. Sobti, A.R. Khan, A. Kandil, F. Murad, P. Friedlander, A.H. Boulares, E. Kandil, Bortezomib sensitizes thyroid cancer to BRAF inhibitor in vitro and in vivo, Endocr. Relat. Cancer 25 (1) (2018) 99–109.
[27] T. Hideshima, H. Ikeda, D. Chauhan, Y. Okawa, N. Raje, K. Podar, C. Mitsiades, N.C. Munshi, P.G. Richardson, R.D. Carrasco, K.C. Anderson, Bortezomib induces canonical nuclear factor-kappaB activation in multiple myeloma cells, Blood 114 (5) (2009) 1046–1052.
[28] J.Z. Qin, J. Ziffra, L. Stennett, B. Bodner, B.K. Bonish, V. Chaturvedi, F. Bennett, P.M. Pollock, J.M. Trent, M.J. Hendrix, P. Rizzo, L. Miele, B.J. Nickoloff, Proteasome inhibitors trigger NOXA-mediated apoptosis in melanoma and myeloma cells, Cancer Res. 65 (14) (2005) 6282–6293.
[29] M. Wang, X.H. Han, L. Zhang, J. Yang, J.F. Qian, Y.K. Shi, L.W. Kwak, J. Romaguera, Q. Yi, Bortezomib is synergistic with rituximab and cyclophosphamide in inducing apoptosis of mantle cell lymphoma cells in vitro and in vivo, Leukemia 22 (1) (2008) 179–185.
[30] J. Ravindran, S. Prasad, B.B. Aggarwal, Curcumin and cancer cells: how many ways can curry kill tumor cells selectively? AAPS J. 11 (3) (2009) 495–510.
[31] P. de la Puente, M.J. Luderer, C. Federico, A. Jin, R.C. Gilson, C. Egbulefu, K. Alhallak, S. Shah, B. Muz, J. Sun, J. King, D. Kohnen, N.N. Salama, S. Achilefu, R. Vij, A.K. Azab, Enhancing proteasome-inhibitory activity and specificity of bortezomib by CD38 targeted nanoparticles in multiple myeloma, J. Control. Release Off. J. Control. Release Soc 270 (2018) 158–176.
[32] X.Y. Pei, Y. Dai, S. Grant, Synergistic induction of oxidative injury and apoptosis in human multiple myeloma cells by the proteasome inhibitor bortezomib and histone deacetylase inhibitors, Clin. Cancer Res. Off. J. Am. Assoc. Cancer Res 10 (11) (2004) 3839–3852.
[33] U. Heider, I. von Metzler, M. Kaiser, M. Rosche, J. Sterz, S. Rotzer, J. Rademacher, C. Jakob, C. Fleissner, U. Kuckelkorn, P.M. Kloetzel, O. Sezer, Synergistic interaction of the histone deacetylase inhibitor SAHA with the proteasome inhibitor bortezomib in mantle cell lymphoma, Eur. J. Haematol. 80 (2) (2008) 133–142.
[34] Y. Dai, S. Chen, L.B. Kramer, V.L. Funk, P. Dent, S. Grant, Interactions between bortezomib and romidepsin and belinostat in chronic lymphocytic leukemia cells, Clin. Cancer Res. Off. J. Am. Assoc. Cancer Res 14 (2) (2008) 549–558.
[35] B. Han, S.H. Liu, W.D. Guo, B. Zhang, J.P. Wang, Y.K. Cao, J. Liu, Notch1 down-regulation combined with interleukin-24 inhibits invasion and migration of hepatocellular carcinoma cells, World J. Gastroenterol. 21 (33) (2015) 9727–9735.
[36] K. Tsumagari, Z.Y. Abd Elmageed, A.B. Sholl, P. Friedlander, M. Abdraboh, M. Xing, A.H. Boulares, E. Kandil, Simultaneous suppression of the MAP kinase and NF-kappaB pathways provides a robust therapeutic potential for thyroid cancer, Cancer Lett. 368 (1) (2015) 46–53.
[37] Q.L. Zhang, L. Wang, Y.W. Zhang, X.X. Jiang, F. Yang, W.L. Wu, A. Janin, Z. Chen, Z.X. Shen, S.J. Chen, W.L. Zhao, The proteasome inhibitor bortezomib interacts synergistically with the histone deacetylase inhibitor suberoylanilide hydroxamic acid to induce T-leukemia/lymphoma cells apoptosis, Leukemia 23 (8) (2009) 1507–1514.
[38] D. Hanahan, R.A. Weinberg, Hallmarks of cancer: the next generation, Cell 144 (5) (2011) 646–674.
[39] J.M. Adams, S. Cory, Bcl-2-regulated apoptosis: mechanism and therapeutic potential, Curr. Opin. Immunol. 19 (5) (2007) 488–496.
[40] F. Chen, A. Pisklakova, M. Li, R. Baz, D.M. Sullivan, Y. Nefedova, Gamma-secretase inhibitor enhances the cytotoxic effect of bortezomib in multiple myeloma, Cell. Oncol. (Dordrecht) 34 (6) (2011) 545–551.
[41] A.L. Penton, L.D. Leonard, N.B. Spinner, Notch signaling in human development and disease, Semin. Cell Dev. Biol. 23 (4) (2012) 450–457.
[42] P. Ntziachristos, J.S. Lim, J. Sage, I. Aifantis, From fly wings to targeted cancer therapies: a centennial for notch signaling, Cancer Cell 25 (3) (2014) 318–334.
[43] M.R. Kamstrup, E. Biskup, L.M. Gjerdrum, E. Ralfkiaer, O. Niazi, R. Gniadecki, The importance of notch signaling in peripheral T-cell lymphomas, Leuk. Lymphoma 55 (3) (2014) 639–644.
[44] D. Guo, Q. Teng, C. Ji, NOTCH and phosphatidylinositide 3-kinase/phosphatase and tensin homolog deleted on chromosome ten/AKT/mammalian target of rapamycin (mTOR) signaling in T-cell development and T-cell acute lymphoblastic leukemia, Leuk. Lymphoma 52 (7) (2011) 1200–1210.
[45] M.G. Cornejo, V. Mabialah, S.M. Sykes, T. Khandan, C. Lo Celso, C.K. Lopez, P. Rivera-Munoz, P. Rameau, Z. Tothova, J.C. Aster, R.A. DePinho, D.T. Scadden, D.G. Gilliland, T. Mercher, Crosstalk between NOTCH and AKT signaling during murine megakaryocyte lineage specification, Blood 118 (5) (2011) 1264–1273.
[46] Z.J. Liu, T. Shirakawa, Y. Li, A. Soma, M. Oka, G.P. Dotto, R.M. Fairman, O.C. Velazquez, M. Herlyn, Regulation of Notch1 and Dll4 by vascular endothelial growth factor in arterial endothelial cells: implications for modulating arteriogenesis and angiogenesis, Mol. Cell. Biol. 23 (1) (2003) 14–25.
[47] M. Dail, J. Wong, J. Lawrence, D. O'Connor, J. Nakitandwe, S.C. Chen, J. Xu, L.B. Lee, K. Akagi, Q. Li, J.C. Aster, W.S. Pear, J.R. Downing, D. Sampath, K. Shannon, Loss of oncogenic Notch1 with resistance to a PI3K inhibitor in T-cell leukaemia, Nature 513 (7519) (2014) 512–516.
[48] A. Baker, D. Wyatt, M. Bocchetta, J. Li, A. Filipovic, A. Green, D.S. Peiffer, S. Fuqua, L. Miele, K.S. Albain, C. Osipo, Notch-1-PTEN-ERK1/2 signaling axis promotes HER2+ breast cancer cell proliferation and stem cell survival, Oncogene 37 (33) (2018) 4489–4504.
[49] G. Dai, S. Deng, W. Guo, L. Yu, J. Yang, S. Zhou, T. Gao, Notch pathway inhibition using DAPT, a gamma-secretase inhibitor (GSI), enhances the antitumor effect of cisplatin in resistant osteosarcoma, Mol. Carcinog. 58 (1) (2019) 3–18.
[50] T. Palomero, A. Ferrando, Oncogenic NOTCH1 control of MYC and PI3K: challenges and opportunities for anti-NOTCH1 therapy in T-cell acute lymphoblastic leukemias and lymphomas, Clin. Cancer Res. Off. J. Am. Assoc. Cancer Res. 14 (17) (2008) 5314–5317.
[51] B. Levine, G. Kroemer, Autophagy in the pathogenesis of disease, Cell 132 (1) (2008) 27–42.
[52] S. Sinha, B. Levine, The autophagy effector Beclin 1: a novel BH3-only protein, Oncogene 27 (Suppl. 1) (2008) S137–S148.
[53] R. Mathew, V. Karantza-Wadsworth, E. White, Role of autophagy in cancer, Nat. Rev. Cancer 7 (12) (2007) 961–967.
[54] J.G. Shelton, W.L. Blalock, E.R. White, L.S. Steelman, J.A. McCubrey, Ability of the activated PI3K/Akt oncoproteins to synergize with MEK1 and induce cell cycle progression and abrogate the cytokine-dependence of hematopoietic cells, Cell Cycle (Georgetown, Tex.) 3 (4) (2004) 503–512.
[55] I. Tremblay, E. Pare, D. Arsenault, M. Douziech, M.J. Boucher, The MEK/ERK pathway promotes NOTCH signalling in pancreatic cancer cells, PLoS One 8 (12) (2013) e85502.
[56] J. Zhang, Z. Wu, A. Savin, M. Yang, Y.R. Hsu, E. Jantuan, J.T.C. Bacani, R.J. Ingham, The c-Jun and JunB transcription factors facilitate the transit of classical Hodgkin lymphoma tumour cells through G1, Sci. Rep. 8 (1) (2018) 16019.
[57] M.H. Lim, I.C. Jeung, J. Jeong, S.J. Yoon, S.H. Lee, J. Park, Y.S. Kang, H. Lee, Y.J. Park, H.G. Lee, S.J. Lee, B.S. Han, N.W. Song, S.C. Lee, J.S. Kim, K.H. Bae, J.K. Min, Graphene oxide induces apoptotic cell death in endothelial cells by activating autophagy via calcium-dependent phosphorylation of c-Jun N-terminal kinases, Acta Biomater. 46 (2016) 191–203.
[58] J. Zhang, Y.M. Su, D. Li, Y. Cui, Z.Z. Huang, J.Y. Wei, Z. Xue, R.P. Pang, X.G. Liu, W.J. Xin, TNF-alpha-mediated JNK activation in the dorsal root ganglion neurons contributes to Bortezomib-induced peripheral neuropathy, Brain Behav. Immun. 38 (2014) 185–191.
[59] C. Yu, M. Rahmani, P. Dent, S. Grant, The hierarchical relationship between MAPK signaling and ROS generation in human leukemia cells undergoing apoptosis in response to the proteasome inhibitor Bortezomib, Exp. Cell Res. 295 (2) (2004) 555–566.